doi: 10.18323/2782-4039-2025-1-71-8

Mathematical modelling to predict the tensile strength of additively manufactured AlSi10Mg alloy using artificial neural networks

Sunita K. Srivastava*[1], researcher
of Department of Mechanical Engineering
N. Rajesh Mathivanan[2], PhD,
professor of Department of Mechanical Engineering
PES University, Bangalore (India)

***E-mail:** sunita.shri45@gmail.com

[1]ORCID: https://orcid.org/0009-0005-2174-2067
[2]ORCID: https://orcid.org/0000-0003-1903-2005

Received 10.09.2024 *Revised 29.10.2024* *Accepted 25.11.2024*

Abstract: Integrating machine learning in additive manufacturing to simulate real manufacturing outcomes can significantly reduce the cost of manufacturing through selective manufacturing. However, limited research exists on developing a prediction model for the mechanical properties of the material. The input variables include key selective laser melting process parameters such as laser power, layer thickness, scan speed, and hatch spacing, with tensile strength as the output. The artificial neural network (ANN) based mathematical model is compared with a second-degree polynomial regression model. The robustness of both models was further assessed with the new data points beyond those used in the development of ANN-based mathematical model and regression model. The results demonstrate that the proposed ANN-based mathematical model offers superior accuracy, with a mean absolute percentage error (MAPE) value of 4.74 % and the R^2 (goodness of fit) value of 0.898 in predicting the strength of AlSi10Mg. The ANN-based mathematical method also demonstrates the strong performance on the new data, achieving a regression value of 0.68. This concludes that the model shows sufficient proof to consider a viable option for predicting the tensile strength.

Keywords: AlSi10Mg alloy; additive manufacturing; artificial neural network (ANN); machine learning; selective laser melting; mathematical model.

For citation: Srivastava S.K., Mathivanan N.R. Mathematical modelling to predict the tensile strength of additively manufactured AlSi10Mg alloy using artificial neural networks. *Frontier Materials & Technologies*, 2025, no. 1, pp. 93–110. DOI: 10.18323/2782-4039-2025-1-71-8.

INTRODUCTION

Additive manufacturing has been the cornerstone of industrial innovation for several decades and has seemingly adapted to handle diverse materials including metal, alloy, polymer, composite, etc. It offers various processes such as binder jetting, fused deposition, powder bed fusion, sheet lamination, material jetting, etc. to meet diverse manufacturing requirements. The fabrication of the metals or composite is majorly done by selective laser melting and laser metal deposition. Additive manufacturing is a preferred manufacturing process for the aluminium alloy and aluminium metal matrix composite for its ability to deliver great accuracy, lesser lead time, cost effectiveness, and superior part qualities compared to conventional manufacturing methods [1]. Pure aluminium however poses challenges during laser melting because of its high reflectivity absorbing only 7 % of the incident laser energy. In contrast, silicon has a high laser absorptivity of around 70 %, which makes aluminium-silicon alloys an ideal candidate for selective laser melting (SLM) due to their enhanced laser absorption [2]. Among the aluminium-silicon alloys, AlSi10Mg stands out as extremely promising because of its excellent mechanical properties and lightweight characteristics. The alloy is very popular in the automobile and aerospace sectors for its exceptional mechanical attributes and remarkable thermal conductivity.

However, the printing parameters of the SLM process such as laser power, layer thickness, scan speed, hatch spacing etc. have a significant impact on the properties of the material, which can be modulated to get the optimum product. For instance, the densification property of the metal can be controlled by varying the laser energy density, which is the combined form of all four process parameters (laser power, layer thickness, scan speed and the hatch spacing). The adjustment helps to achieve the desired mechanical properties of the metal such as tensile strength, compressive strength, hardness, and microhardness, etc. [3].

Machine learning, which is the subset of artificial intelligence plays a vital role in generating a model/system by enabling automatic learning from the provided data and improving the accuracy without any extensive programming [4].

Within this realm, an artificial neural network (ANN), a part of deep learning, mimics the working principle of a human brain. It has interconnected nodes within its

architecture that simulate the biological neurons. The ANN architecture comprises of input layers (comprising independent variables), hidden layers (comprising one or more) and output layers (comprising dependent variables). Each node of a layer is connected to the next set of nodes through weights, biases and a transfer function to send the signal. ANN uses the training data to establish the connection between input and output. It learns and fine-tunes the accuracy of the model through iterative learning which makes it a very powerful tool in the domain of artificial intelligence [5]. The basic ANN architecture used in this study is depicted in the Fig. 1.

This model can be used for the prediction of unknowns and for finding optimal solutions by analysing the influence of input parameters. However, there are very few studies have been performed in this area.

Shubham et al. [6] assessed six different machine learning models such as deep learning, bagging, decision tree, linear regression, random forest and ridge regression to evaluate the influence of manufacturing parameters such as laser power, scan speed, scan space, and island size on the tensile strength of AlSi10Mg alloy. It was concluded that deep learning and decision trees can have prediction accuracy of up to 99 and 89 % respectively. It was also highlighted that laser power is the most influencing parameter among all the four parameters considered. Ghetiya et al. [7] explored the machine learning approach to optimise the process parameters of friction stir welding of aluminium plates. The input welding parameters considered are tool rotational speed, welding speed, tool shoulder diameter and axial force. An ANN model was developed utilising a backpropagation algorithm to predict the tensile strength for the given process parameters. The results show a good alignment of the model with the experimental values and can be used as an alternate way to calculate the tensile strength.

M. Khalefa [8] developed the ANN model from the experimental data of stir-casting manufactured Al–Si alloy. The application of the model is to predict the effect of silicon content on tensile strength, hardness, and wear loss. The obtained results exhibit that the predicted values satisfactorily align with the experimental values with mean square error (MSE) of 0.0335, 0.0023, and 0.014 for the tensile test, the hardness test, and the wear loss respectively. Alamri et al. [9] explored the prediction of the part quality that includes assessing relative density, surface roughness, and hardness in relation to laser power, hatch spacing, scan velocity and layer thickness of selective laser melting manufactured AlSi10Mg alloy. This study has used five different supervised learning algorithms such as artificial neural network (ANN), support vector regression (SVR), kernel ridge regression (KRR), random forest (RF), and Lasso regression to compare the results. The ANN was found to be outperformed among other models based on computation results. Additionally, laser power and scan speed emerged as the predominant parameters influencing relative density and hardness, while layer thickness and scan speed impact the surface roughness the most.

Given limited research, this study develops a novel approach to integrate an ANN-based mathematical model and regression model to predict the tensile strength of additively manufactured (SLM) AlSi10Mg alloys based on available data.

The emphasis of the study is on the development of a correlation between tensile strength and selective laser melting parameters such as laser power, layer thickness, scan speed, and hatch spacing. Furthermore, this research contributes valuable insight into using a machine learning model to predict material properties without the need of actual experimentation.

The objective of this work is to enhance the ability to predict and optimise the material properties from the experimental data and to provide better control over the production process, through a reliable predictive model.

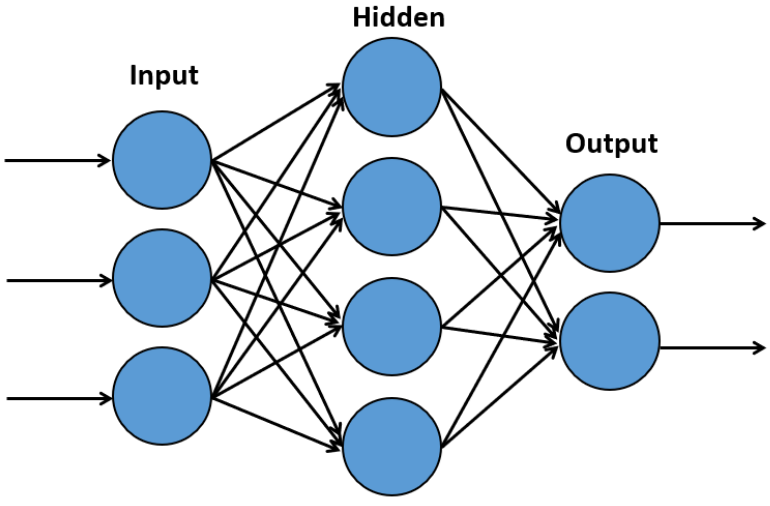

Fig. 1. *Architecture of an artificial neural network*
Рис. 1. *Архитектура искусственной нейронной сети*

The work aims to support a more cost and time effective approach for the material assessment. In doing so, this study lays a foundation for future research by integrating machine learning and neural network models into additive manufacturing.

METHODS

Data collection for the artificial neural network and regression model

The input dataset for the ANN and regression models are gathered from the existing literature for the as-built AlSi10Mg sample fabricated via a selective laser melting process. Additionally, a new experiment was conducted in this study as part of data collection for the ANN model. The ANN model and regression model were developed using 108 data points (Appendix 1) and a further 27 data points (Appendix 2) were used to assess the precision of the model selected randomly. The model's predicted output was compared with the experimental value reported in the literature. Both the artificial neural network and regression models were implemented using MATLAB R2023b. The model utilises the laser power denoted by (P), layer thickness denoted (T), scan speed denoted by (V), and hatch spacing denoted by (H) as the input variables. The input data range for the ANN model was taken as 150–1000 W for laser power, 20–80 μm for layer thickness, 195–2400 mm/s for the scan speed, and 42–240 μm for hatch spacing.

Experiment

The gas-atomised AlSi10Mg powder of average particle size range 20–63 μm was used in the manufacturing which primarily consists of up to 10 % silicon, a trace amount of magnesium and iron. The detailed composition of the powder is shown in Table 1.

The samples were fabricated using the SLM process in RenAM 500E machine (UK). The key manufacturing parameters of the manufacturing include laser power is 275 W, layer thickness is 30 μm, scanning speed is 2000 mm/s and hatch distance is 80 μm. The build chamber was filled with 99.999 % pure argon gas to protect from the oxidation of the powder. The building direction has been kept horizontal and the layers were oriented to an angle of 67° from the preceding layer. The temperature of the build plate was maintained at 80 °C initially to avoid failure due to the change in temperature between the bottom layer and the building plate.

The flat-type sub-size tensile test specimens of gauge length 25 mm were manufactured following the ASTM E8 standard as shown in Fig. 2. The as-built components were kept at stress relieved at 300±10 °C for 2 h and air cooled.

Tensile tests were conducted on the universal testing machine, model ETM (Wance, China) of 50 kN capacity at a strain rate of 1 mm/min. The axial displacement was monitored by a computer integrated video extensometer connected to a tensile testing machine which captures real-time elongation data to construct the stress–strain diagram.

The yield strength was determined using the 0.2 % offset method using the stress–strain Excel graph. First, the linear (elastic) region of the stress-strain graph was identified to determine the slope (elastic modulus). A line was then drawn parallel to this linear part of the graph, passing through 0.2 % of the strain (Y-axis). The yield strength is defined as the point where the offset line intersects the stress–strain curve.

Development of an artificial neural network

MATLAB R2023b version was used to implement the ANN model using the neural network fitting tool within the deep learning toolbox. A supervised machine learning approach was employed to predict the strength of the material. The training was run for the target epoch value of 1000 with four input variables (laser power, layer thickness, scan speed/velocity, and hatch spacing/distance) and two outputs (yield and tensile strength).

It is worth noting that the neural network uses two two-layer feedforward designs. The input layer and output layer use hyperbolic tangent (tansig) and liner (purelin) transfer function respectively as shown in Fig. 3.

The neural network structure consists of 10 neurons in the hidden layers and 2 neurons corresponding to the output variables. This configuration is selected based on the complexity and performance requirements of the ANN model. The hidden layer is designed to effectively extract features from the input layers. A common approach to determine the number of neurons in the hidden layer is to double the number of neurons in the input layer and add the number of neurons in the output layer[1].

The adopted data is categorised into three different categories randomly training, validation, and testing in 80:10:10 ratio. The Levenberg–Marquardt algorithm (trainlm) is used for the training of the ANN model, which is often considered the fastest back-propagation algorithm. The input and output data are normalised between −1 and +1 to achieve dimensional consistency and to achieve compatibility with tansig transfer function using equation (1) [10]:

$$M_{norm} = \frac{2 \times (N_i - N_{\min})}{N_{\max} - N_{\min}} - 1, \quad (1)$$

where M_{norm} is normalised parameters;
N_i is actual data;
N_{min} and N_{max} are the minimum and maximum values of the actual data respectively.

Polynomial regression analysis

A multivariate polynomial regression model was created using MATLAB to create the correlation between the dependent variable (ultimate tensile strength) and independent variables (laser power, layer thickness, scan speed/velocity, and hatch spacing/distance). The same experimental results that were used to develop the ANN model are utilised for

[1] *Livshin I. Artificial Neural Networks with Java: Tools for Building Neural Network Applications. Chicago, 2019. 575 p. DOI: 10.1007/978-1-4842-4421-0.*

Table 1. *Composition of AlSi10Mg powder*
Таблица 1. *Состав порошка AlSi10Mg*

Element	Al	Si	Mg	Fe	N	O	Ti	Zn	Mn	Ni	Cu	Pb	Sn
Mass. %	Balance	9–11	0.25–0.45	<0.25	<0.20	<0.20	<0.15	<0.10	<0.10	<0.05	<0.05	<0.02	<0.02

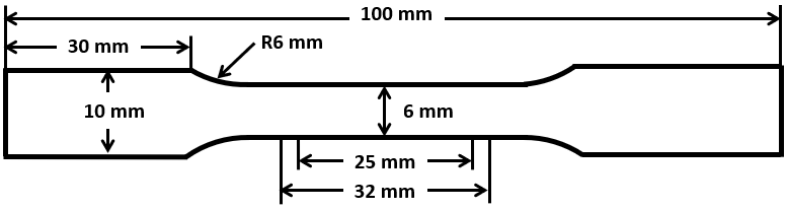

a

b

Fig. 2. *Sample details:* ***a*** *– sample dimension;* ***b*** *– fabricated sample*
Рис. 2. *Параметры образца:* ***a*** *– размеры;* ***b*** *– образец*

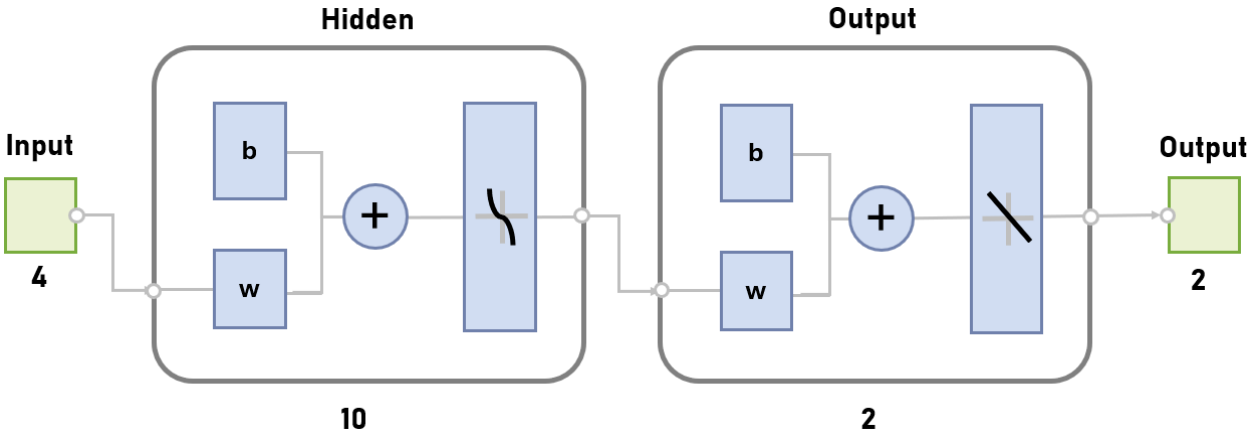

Fig. 3. *Network architecture*
Рис. 3. *Архитектура сети*

the multivariate regression model. The multi-variant polynomial regression, *fitlm* facilitates the modelling of the relation between multiple input predictors and a single response. The model computes coefficients for each set of variables and the intercept terms. It determines the impact of each predictor on the response variable. The second-degree polynomial function is calculated using statistics and machine learning toolbox:

$$Y(X) = a_0 + \sum_{i=0}^{N} a_i X_i + \\ + \sum_{i<j}^{N} a_{ij} X_i X_j + \sum_{i=0}^{N} a_{ij} X_i^2 , \quad (2)$$

where Y is the predicted response;

a_0 is the intercept coefficient;

$a_i X_i$ are the linear terms;

$a_{ij} X_i X_j$ are the interaction terms;

$a_{ij} X_i^2$ are the square terms.

RESULTS

Experimental values

The tensile test of the SLM fabricated specimen is performed as per ASTM E8 standard and results are presented in the Table 2. In the tensile test, the specimen is broken in the direction perpendicular to the applied force as shown in Fig. 4. The tensile strength of the specimen is reported as 436.95 MPa at the maximum force of 15.7 KN and the specimen exhibits an elongation of 9.59 %. The failure of the specimen is identified as brittle and sudden occurring before the material entered the plastic zone as shown in stress–strain diagram (Fig. 5). The yield strength was found to be 58 MPa, calculated using the 0.2 % proof/offset method.

Artificial neural network results

The performance of the developed ANN is assessed using various evaluations and analytical metrics. The comprehensive output of the ANN is shown in Table 3.

ANN regression plot for overall training, validation, and test data for yield and tensile strength is shown in Fig. 6. The *X*-axis represents the value of the target (experimental data) and the *Y*-axis shows the output data predicted using the ANN model. The dotted line illustrates the ideal correlation where actual and predicted values are equal, while the solid line represents the actual/true correlation between the *X* and *Y* axis.

It is observed that the correlation coefficient (*R*-value) for the overall output of the training, validation, and test data is 0.96, 0.94, and 0.91 respectively. The overall *R*-value is 0.96 which shows a strong correlation between actual (target) and predicted output.

The value at which MSE between actual and predicted values converges is shown by the best validation of the performance curve. The back-propagation algorithm calibrates the values of weights and biases with each iteration and generates the lowest MSE value. The number of epochs represents the number of iterations performed by the network to converge it to a minimum [11]. The performance curve of this study is shown in Fig. 7, which shows the best performance of the model of value 0.024 at epoch 44. From the performance curve, it was evident that there is no over-fitting observed. Additionally, similar trends have been observed for training, testing, and validation data.

Table 2. *Tensile test results*
Таблица 2. *Результаты испытаний на растяжение*

Mechanical properties	Values
Yield stress, MPa	58
Tensile strength, MPa	436.95
Elongation, %	9.59
Maximum force, KN	15.73

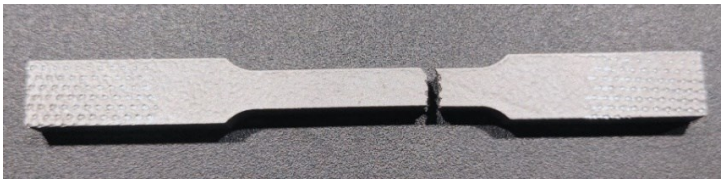

Fig. 4. *Fractured sample*
Рис. 4. *Разрушенный образец*

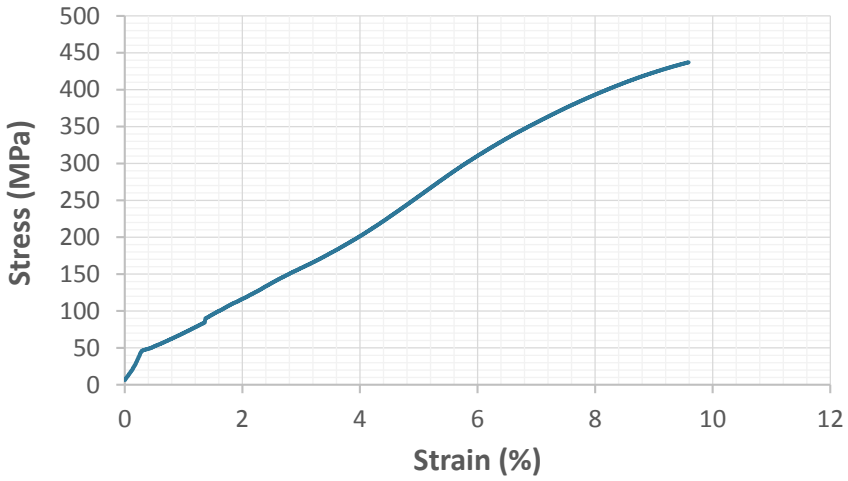

Fig. 5. *Stress–strain diagram*
Рис. 5. *Диаграмма «напряжение – деформация»*

Table 3. *Artificial neural network output*
Таблица 3. *Выходные данные искусственной нейронной сети*

ANN output	Value
Epoch value	50
R-value – training	0.96
R-value – validation	0.94
R-value – test	0.91
R-value – all	0.96
MSE	0.0155

Development of mathematical formula based on ANN

Once the ANN model is trained it can be translated into a mathematical equation or model by integrating transfer function using weights and biases as depicted in equation [10]:

$$Y = b_0 + \sum_{k=1}^{h}\left(w_k \times f_{sig}\left(b_{hk} + \sum_{k=1}^{m} w_{ik} X_i\right)\right), \quad (3)$$

where Y is the normalised output variables;
b_0 is the bias at the output layer;
w_k is the weight that connects between the *kth* hidden layer and the single output neuron;
b_{hk} is the bias at the *kth* neuron of the hidden layer;
h and m are the number of neurons in the hidden layer and input layers, respectively;
w_{ik} is the connection weight between the *ith* input variable and the hidden layer;
X_i is the normalised input variable;
f_{sig} is the transfer function used to train the ANN.

The number of neurons connected to the input and hidden layer is h=10. The adopted transfer function between the input and output layers is *tansig* (f_{sig} = *tansig)* and *purelin* respectively.

Therefore, the equation (3) can be converted into equation [12]:

$$TS_n = -0.0825 + [W] \times [q]^T, \quad (4)$$

where TS_n is the normalised tensile strength;

$$[W] = [1.279 - 0.1180\ 0.6628 - 2.9155\ 2.6693 - 2.8315 - 0.3615\ 3.2800\ 0.7236 - 1.8831];$$

$$[q] = [\tanh A_1 \tanh A_2 \tanh A_3 \tanh A_4 \tanh A_5 \tanh A_6 \tanh A_7 \tanh A_8 \tanh A_9 \tanh A_{10}];$$

$$\tanh = f(x) = \frac{e^x - e^{-x}}{e^x + e^{-x}}.$$

The normalised variables A_1 to A_{10} can be calculated using matrix equations:

$$\begin{bmatrix} A_1 \\ A_2 \\ A_3 \\ A_4 \\ A_5 \\ A_6 \\ A_7 \\ A_8 \\ A_9 \\ A_{10} \end{bmatrix} = \begin{bmatrix} 0.4549 & -0.2335 & 1.5844 & -1.7360 \\ 0.6977 & 0.1801 & 4.0404 & 3.2143 \\ 0.5458 & 5.7727 & 4.3710 & -6.2395 \\ -1.9850 & -0.4610 & 1.2824 & -0.8306 \\ -4.5821 & 0.2266 & 1.3249 & -1.1109 \\ -2.520 & 5.4207 & 1.8587 & 0.2827 \\ -0.4423 & 0.1586 & -0.5219 & 3.0538 \\ -0.9543 & 2.7184 & 0.4837 & 0.6755 \\ 1.6739 & -2.8579 & 0.3978 & 2.3733 \\ 1.2295 & 3.2789 & -2.5835 & 1.1224 \end{bmatrix} \begin{bmatrix} P \\ T \\ V \\ H \end{bmatrix} + \begin{bmatrix} -2.5042 \\ 1.6432 \\ 4.3932 \\ -0.6902 \\ -1.3171 \\ -0.7925 \\ 0.3307 \\ -0.6097 \\ -0.9304 \\ -2.5837 \end{bmatrix}.$$

The normalised tensile strength in equation (4) needs to be de-normalised to derive the required predictive mathematical equation. The de-normalised equation to predict the tensile strength is shown in equation (5):

$$TS_d = \frac{(TS_n + 1) \times 318.8}{2} + 160, \qquad (5)$$

where TS_d is the de-normalised tensile strength, the minimum and maximum values of input tensile strength are 160 and 478.8 MPa respectively.

Hence equation (5) represents the ANN-based mathematical model to predict the tensile strength for the provided value of laser power, layer thickness, scan speed, and hatch spacing.

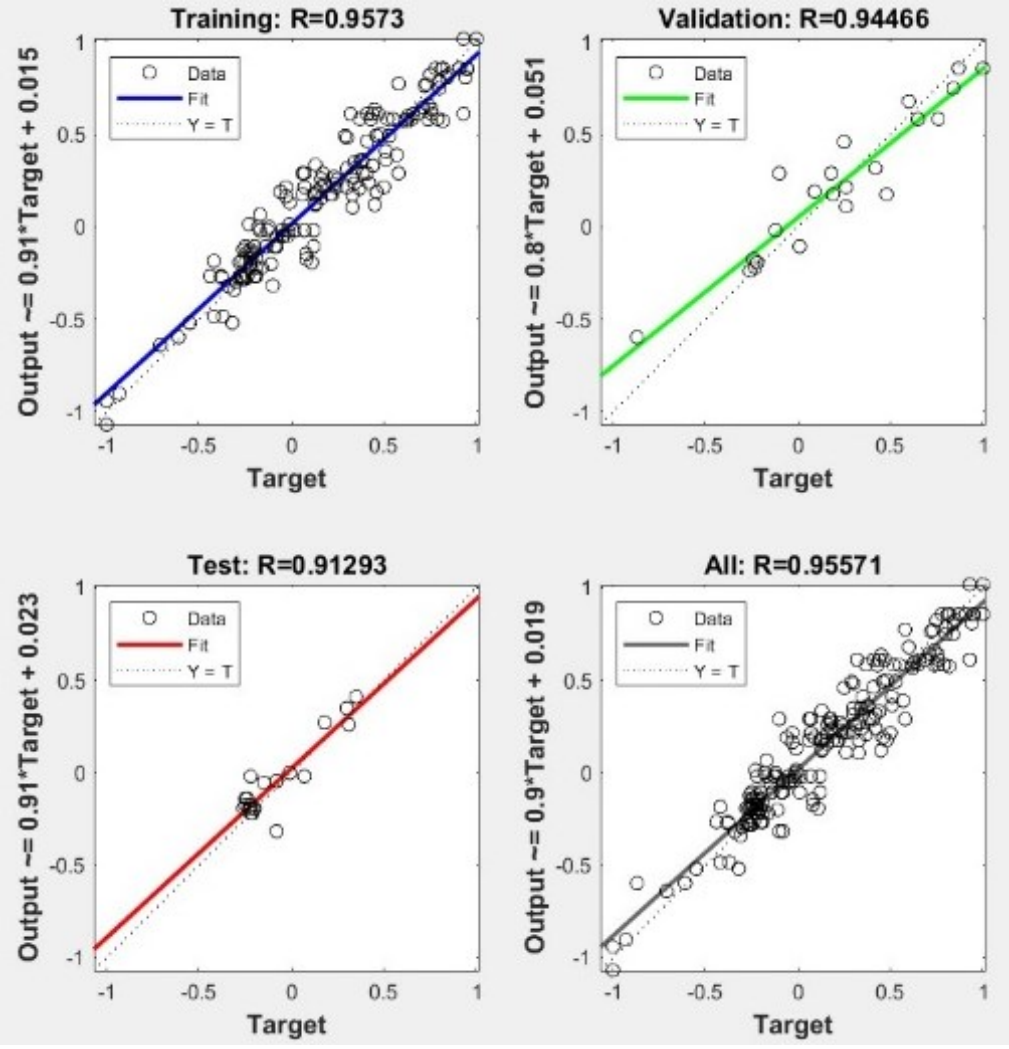

Fig. 6. *Regression plot*
Рис. 6. *График регрессии*

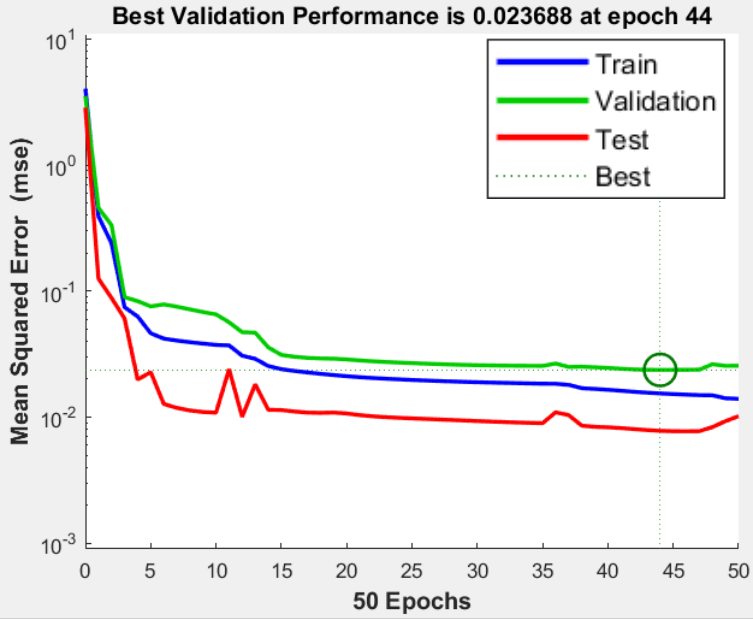

Fig. 7. *Performance plot*
Рис. 7. *График эффективности*

Polynomial regression analysis using MATLAB

The experimental results are fitted in the quadratic equation (2) resulting in the proposed regression model as shown in equation:

$$\begin{aligned} T.S = & -33.83 + 3.1866 \times P - 0.0435 \times T + 0.2681 \times V - \\ & - 2.9162 \times H - 0.0313 \times P \times T - 0.0004 \times P \times V - \\ & - 0.0182 \times P \times H - 0.0068 \times T \times V + \\ & + 0.1159 \times T \times H + 0.0025 \times V \times H + 0.0005 \times P^2 + \\ & + 0.0186 \times T^2 - 0.0001 \times V^2 + 0.0045 \times H^2 \end{aligned}, \quad (6)$$

where $T.S$ is the tensile strength;
P is the laser power;
T is the layer thickness;
V is the scan speed;
H is the hatch spacing.

DISCUSSION

Validation of mathematical formula based on ANN

The comparison between ANN predicted output and mathematical model predicted output is plotted in Fig. 8. Evidently, the proposed mathematical model replicates the ANN output perfectly with a goodness of fit of (R^2)=1 and can be used to predict the tensile strength without running the ANN model. Fig. 9 shows the trend comparison between actual experimental values and predicted output. The mean absolute percentage error (MAPE) between the experimental and predicted value stands at 4.74 % which demonstrates quite a good accuracy. The goodness of fit (R^2) between the ANN predicted data and actual experimental value is 0.898 (Fig. 10 a). This indicates that the predicted value matches the actual value by 89.8 %.

Validation of regression model

The calculated goodness of fit between the experimental value and predicted value using the polynomial regression model is 0.68, which means the predicted value aligns with the experimental value with an accuracy of 68 %, as shown in Fig. 10 b.

Additionally, the mean absolute percentage error (MAPE) calculated between experimental and predicted values are 8.83 %, which shows a moderate level of deviation with respect to experimental values. Fig. 11 shows the trend comparison between actual and predicted values.

***F*-test and standard error of the regression coefficients**

The *F*-test of the regression model is performed to assess the predictive power and the significance of the relationship between dependent and independent variables using equations from:

$$SST = \sum \left(Y_i - \overline{Y}\right)^2;$$

$$SSR = \sum \left(\hat{Y}_i - \overline{Y}\right)^2;$$

$$SSE = \sum \left(Y_i - \hat{Y}_i^{\,2}\right);$$

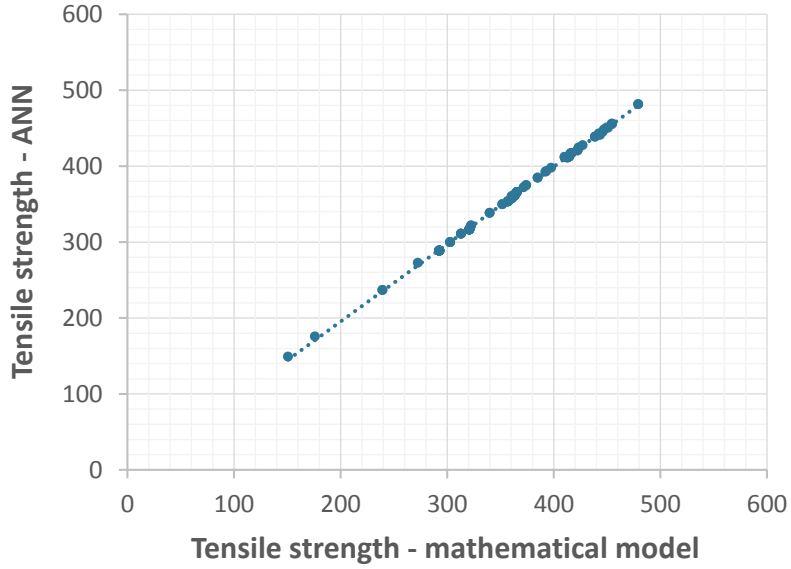

Fig. 8. *Tensile strength predicted using ANN vs mathematical model*
Рис. 8. *Предел прочности, рассчитанный с помощью ИНС и математической модели*

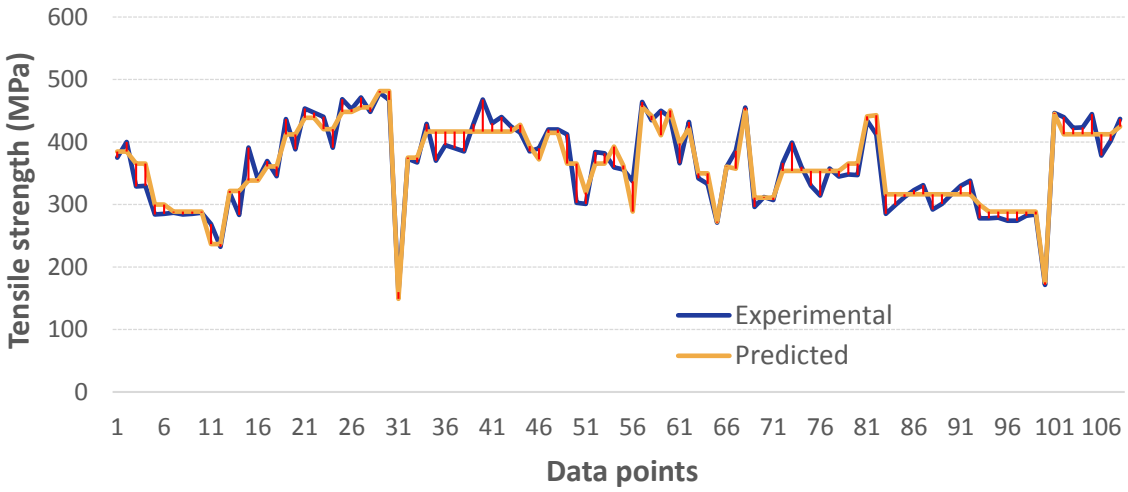

Fig. 9. *Experimental vs predicted values of tensile strength (ANN)*
Рис. 9. *Экспериментальные и спрогнозированные значения предела прочности (ИНС)*

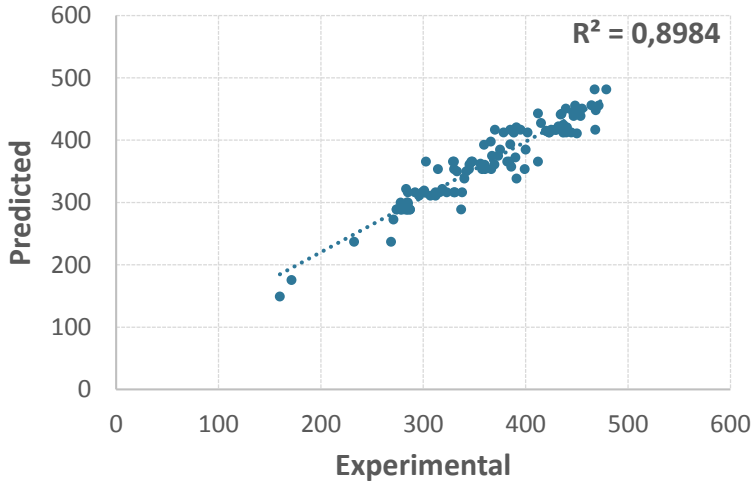

a

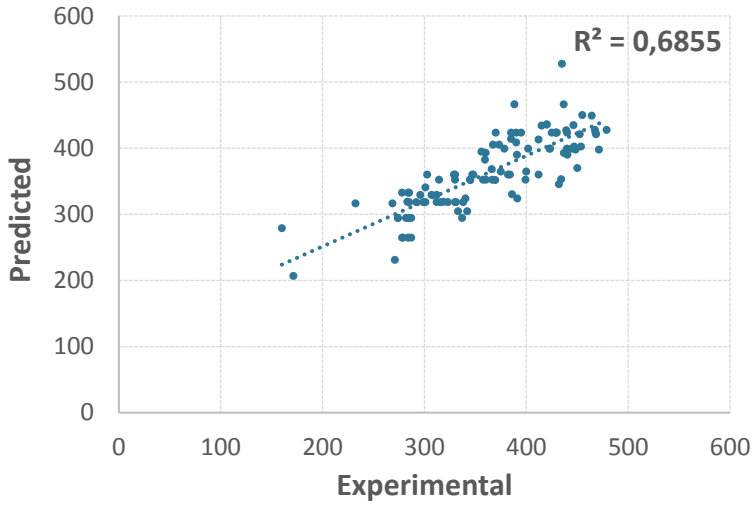

b

Fig. 10. *Comparison of the measured vs predicted tensile strength:*
a *– ANN-based model;* ***b*** *– polynomial regression model*
Рис. 10. *Сравнение экспериментального и спрогнозированного предела прочности:*
a *– модель на основе ИНС;* ***b*** *– модель полиномиальной регрессии*

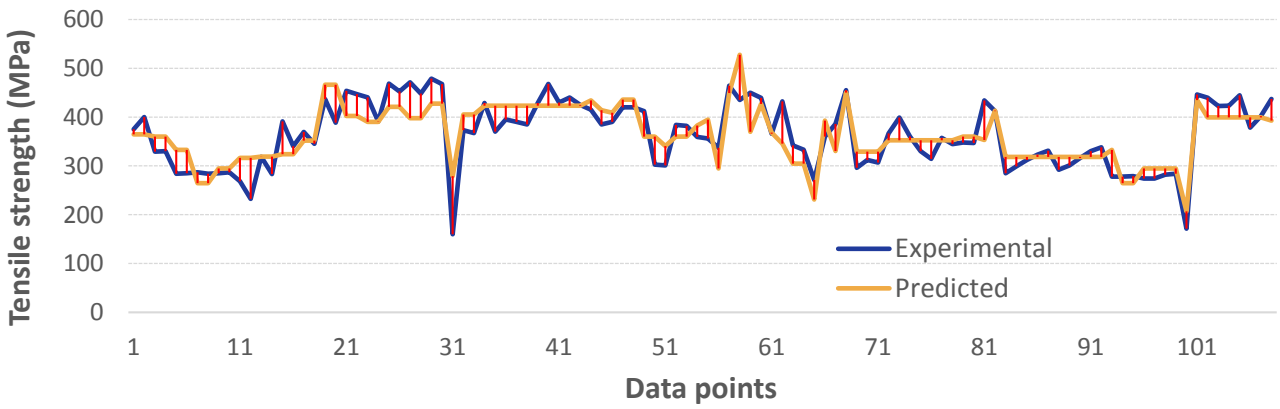

Fig. 11. *Experimental vs predicted values of tensile strength (polynomial regression)*
Рис. 11. *Экспериментальные и спрогнозированные значения предела прочности (полиномиальная регрессия)*

$$MSR = \frac{SSR}{k};$$

$$MSE = \frac{SSE}{n-k-1};$$

$$F-statistic = \frac{MSR}{MSE},$$

where SST is total sum of squares;
SSR is regression sum of squares;
SSE is residual sum of squares;
MSR is mean square for regression;
MSE is mean square for error;
Y_i is experimental values;
$\overline{Y}$ is mean of experimental values;
$\hat{Y}_i$ is predicted values;
k is No of independent variable;
$n-k-1$ is degrees of freedom.

Since F calculated 13.36>$F_{critical}$ at the 0.05 significance level, there is statistically significant relationship between the predictor and response variable.

The standard error of the regression coefficient measures the variability of the estimated coefficients if the study were repeated. It measures the uncertainty associated with the regression model and how much it is expected to vary due to sampling variability. The analysis is performed using MATLAB using equations:

$$X = \begin{bmatrix} 1 & P_1 & T_1 & V_1 & H_1 & P_1T_1 & P_1V_1 \\ 1 & P_2 & T_2 & V_2 & H_2 & P_2T_2 & P_2V_2 \\ . & . & . & . & . & . & . \\ . & . & . & . & . & . & . \\ 1 & P_n & T_n & V_n & H_n & P_nT_n & P_nV_n \end{bmatrix};$$

$$\begin{bmatrix} P_1H_1 & T_1V_1 & T_1H_1 & V_1H_1 & P_1^2 & T_1^2 & V_1^2 & H_1^2 \\ P_1H_2 & T_2V_2 & T_2H_2 & V_2H_2 & P_2^2 & T_2^2 & V_2^2 & H_2^2 \\ . & . & . & . & . & . & . & . \\ . & . & . & . & . & . & . & . \\ P_nH_n & T_nV_n & T_nH_n & V_2H_2 & P_n^2 & T_n^2 & V_n^2 & H_n^2 \end{bmatrix}$$

$$\text{Residual Variance, } \sigma^2 = \frac{SSR}{n-p};$$

Variance – Covariance Matrix of Coefficients,

$$\text{Var}\left(\hat{\beta}\right) = \sigma^2\left(X'X\right)^{-1}.$$

The standard errors are the square roots of the diagonal elements of variance-covariance matrix:

Standard error of Coefficients

$$\text{SE}\left(\hat{\beta}\right) = \sqrt{\text{diag}\left(\text{Var}\left(\hat{\beta}\right)\right)}.$$

The result of the study is summarised in Table 4. As stated, the standard error of the coefficient provides the measure of uncertainty of the coefficients. The relatively small error indicates the precise estimate and significance of the impact of the coefficient as seen for the variables V, V^2, P^2, T^2, H^2, $P{\cdot}T$, $P{\cdot}V$, $P{\cdot}H$, $T{\cdot}V$, and $V{\cdot}H$. In contrast, the relatively large standard error for the variable T and the intercept suggest that the estimations are not very precise and likely to vary more across the samples.

Validation of proposed models with the new data sets

ANN-based mathematical and polynomial regression models are validated on the new set of 27 data points, the datasets beyond those that are used in the model development. The experimental values of the data points are collected from the previous literature. ANN-based mathematical equation (5) and polynomial regression equation (6) were used for the prediction of the tensile strength of the new input datasets and the same was compared with the experimental values to assess the robustness of the model. The validation was done using statistical parameters such as goodness of fit (R-square) to measure how well the model fits the data, mean absolute percentage error (MAPE) to provide the relative accuracy of the prediction, mean absolute error (MAE) to measure overall prediction error and root mean squared error (RMSE) to find out the impact of the larger error as outlined in equations:

$$R^2 = 1 - \frac{\text{Sum of squares of residuals}}{\text{Total sum of squares}};$$

$$\text{Mean absolute percentage error (MAPE)} = \frac{1}{n}\sum\frac{\text{Prediction} - \text{Actual}}{\text{Actual}} \times 100;$$

$$\text{Mean absolute error (MAE)} = \frac{1}{n}\sum\left|\text{Prediction} - \text{Actual}\right|;$$

$$\text{Root Mean Square Error (RMSE)} = \sqrt{\frac{\sum\left(\text{Prediction} - \text{Actual}\right)^2}{n}}.$$

Fig. 12 illustrates the comparison of experimental values with an ANN-based mathematical model and polynomial regression model. The mean error percentage was found to be 11.1 and 16.8 % for ANN-based equation and polynomial regression model respectively. The summary of the validation of the two models is shown in Table 5.

Comparison and validation with prior research

The experimental results of tensile properties assessment of SLM fabricated AlSi10Mg sample demonstrate strong consistency with the previous studies [13–17].

Table 4. *Standard error of a regression coefficient*
Таблица 4. *Среднее квадратическое отклонение коэффициента регрессии*

Variable	Coefficient	Standard errors of the regression
Intercept	−33.83	156.8213
P	3.1866	0.5771
T	−0.0435	4.3601
V	0.2681	0.0783
H	−2.9162	0.741
$P{\cdot}T$	−0.0313	0.006
$P{\cdot}V$	−0.0004	0.0002
$P{\cdot}H$	−0.0182	0.0024
$T{\cdot}V$	−0.0068	0.0015
$T{\cdot}H$	0.1159	0.0134
$V{\cdot}H$	0.0025	0.0007
P^2	0.0005	0.0003
T^2	0.0186	0.0397
V^2	−0.0001	0
H^2	0.0045	0.0022

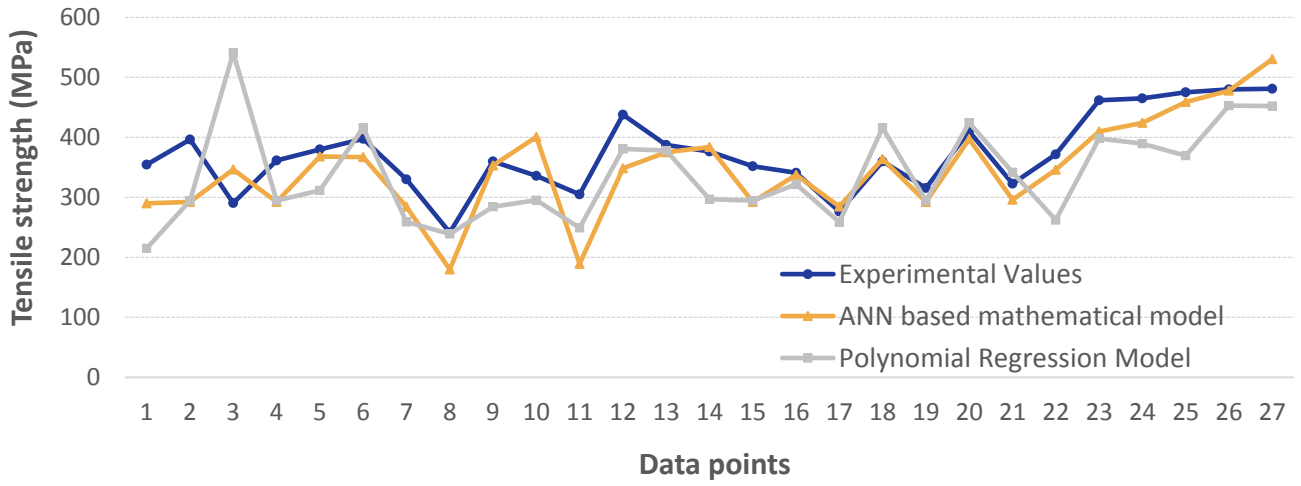

Fig. 12. *Experimental vs predicted values of tensile strength for new data points*
Рис. 12. *Экспериментальные и спрогнозированные значения предела прочности для новых точек данных*

Table 5. *Summary of the validation of ANN-based and regression models*
Таблица 5. *Результат оценки модели на основе ИНС и регрессионной модели*

Evaluation metric	ANN based mathematical model	Polynomial regression model
R-square (R^2)	0.68	0.25
Mean absolute error (MAE)	39.44	61.17
Mean absolute percentage error (MAPE)	11.10	16.89
Root mean square error (RMSE)	50.37	79.28

The tested specimen exhibited significantly higher tensile strength approximately 25 % higher than that of conventionally cast specimens [18].

The developed ANN model and regression model clearly show the dependency of the output on the key process parameters i. e. laser power, layer thickness, hatch spacing, and scan speed. The observation aligns with the previous studies, which identified the laser power and scan speed as the common predominant influencing factors on the material properties [6; 9].

The results clearly show that the ANN model outperformed the regression model, showing superior predictability for the material properties. This aligns with previous studies, that highlight the ability of the ANN model to handle complex, multi-functional, non-linear relationships [6; 9; 19]. For example, M. Khalefa [8] achieved an MSE of 0.0335 for tensile strength prediction using ANN, while other researchers [9] reported MSE values of 0.232, 0.395, 0.122 for relative density, surface roughness, and hardness respectively. Similarly, Ghetiya et al. [7] achieved the MSE value less than 3 % using an ANN model for tensile strength prediction. In this study, the accuracy of the ANN surpasses some earlier findings by predicting material properties with an MSE value of 0.0155 and an overall R value of 0.96. This improvement is attributed to the use of a wider range of datasets for model training, which enhances its reliability and provides a comprehensive representation of the problem [20].

Contributions and implications of the study

The current study contributes to the additive manufacturing field by providing a precise machine learning based approach for the prediction of material properties using input process parameters. The work narrows down on the prediction of tensile strength of SLM manufactured AlSi10Mg alloy, offering a useful tool for manufacturing and design engineers.

This finding also offers a practical and efficient solution by minimising manufacturing time and resource usage. By enabling the real time optimisation of manufacturing costs, the research supports the production of high-quality parts.

Furthermore, as the machine learning model is trained to predict the properties under various conditions, the study also provides further advancements in this area by encouraging input parameters optimisation to reduce material defects through the correlation between the inputs and outputs.

The study presents a boarder implication as it empowers the adoption and integration of machine learning applications in additive manufacturing. The work further promotes the artificial intelligence, data driven approach in advanced material properties optimisation.

Limitation of proposed ANN model

The proposed ANN model comes with certain limitations as follows:

1. The input variables should fall within the range of minimum and maximum range of the variables used in the development of the ANN model.

2. The input and output should be normalised using equation (1) before feeding it into the ANN model.

3. ANN is a complex system compared to the regression model, which requires more computational resources. ANN typically requires more datasets to train the model effectively. The availability of a limited experimental dataset can limit the capability of the ANN and cause overfitting.

CONCLUSIONS

In this study an artificial neural network model is adapted as a mathematical equation model and a regression model is developed to predict the tensile strength of additively manufactured (SLM) AlSi10Mg alloy based on existing experimental data. The effectiveness of the ANN-based mathematical model is then evaluated and compared to the regression model on the datasets distinct from those used in the model development. The following conclusion can be drawn from the study:

1. The proposed ANN-based mathematical model exhibits superior performance compared to the regression model with the R^2 (goodness of fit) value of 0.898 against 0.685 of the regression value for the input data sets used for the model development. The ANN-based mathematical model also performed comparatively well for the new datasets yielding a regression value of R^2 as 0.68.

2. Notably, the ANN-based mathematical model demonstrates low mean absolute percentage error of 4.74, and 11.1 % for the datasets used for model development and the new input data-sets respectively.

3. This concludes that the accuracy of the ANN-based mathematical model is good enough to consider it as

the viable option for the prediction. However, the efficacy of the ANN model is limited for the new input datasets, because of the limited data availability. The inclusion of more datasets into the development and validation of the ANN model is expected to bring more accuracy. Exploring various neural network techniques and fine tuning the hyperparameters can improve the model performance further.

REFERENCES

1. Rouf S., Malik A., Singh N., Raina A., Naveed N., Siddiqui M.I.H., Haq M.I.Ul. Additive manufacturing technologies: Industrial and medical applications. *Sustainable Operations and Computers*, 2022, vol. 3, pp. 258–274. DOI: 10.1016/j.susoc.2022.05.001.
2. Sercombe T.B., Li X. Selective laser melting of aluminium and aluminium metal matrix composites: review. *Materials Technology*, 2016, vol. 31, no. 2, pp. 77–85. DOI: 10.1179/1753555715Y.0000000078.
3. Chowdhury S., Yadaiah N., Prakash Ch., Ramakrishna S., Dixit S., Gulta L.R., Buddhi D. Laser Powder Bed Fusion: A State-of-the-Art Review of the Technology, Materials, Properties & Defects, and Numerical Modelling. *Journal of Materials Research and Technology*, 2022, vol. 20, pp. 2109–2172. DOI: 10.1016/j.jmrt.2022.07.121.
4. Xu Yongjun, Liu Xin, Cao Xin et al. Artificial intelligence: A powerful paradigm for scientific research. *The Innovation*, 2021, vol. 2, no. 4, article number 100179. DOI: 10.1016/j.xinn.2021.100179.
5. Osman E.-S., Aggour M.A. Artificial neural network model for accurate prediction of pressure drop in horizontal and near-horizontal-multiphase flow. *Petroleum Science and Technology*, 2002, vol. 20, no. 1-2, pp. 1–15. DOI: 10.1081/LFT-120002082.
6. Shubham P., Sharma A., Vishwakarma P.N., Phanden R.K. Predicting Strength of Selective Laser Melting 3D Printed AlSi10Mg Alloy Parts by Machine Learning Models. *8th International Conference on Signal Processing and Integrated Networks (SPIN)*. India, 2021, pp. 745–749. DOI: 10.1109/SPIN52536.2021.9566142.
7. Ghetiya N.D., Patel K.M. Prediction of Tensile Strength in Friction Stir Welded Aluminium Alloy Using Artificial Neural Network. *Procedia Technology*, 2014, vol. 14, pp. 274–281. DOI: 10.1016/j.protcy.2014.08.036.
8. Khalefa M. Use of artificial neural network for prediction of mechanical properties of Al–Si alloys synthesized by stir casting. *Journal of Petroleum and Mining Engineering*, 2019, vol. 21, pp. 97–103. DOI: 10.21608/jpme.2019.13857.1004.
9. Alamri F., Maalouf M., Barsoum I. *Prediction of Porosity, Hardness and Surface Roughness in Additive Manufactured AlSi10Mg Samples: preprint*. 2023. DOI: 10.21203/rs.3.rs-3186551/v1.
10. Lawal A.I., Aladejari A.E., Onifade M., Bada S., Idris M.A. Predictions of elemental composition of coal and biomass from their proximate analyses using ANFIS, ANN and MLR. *International Journal of Coal Science and Technology*, 2024, vol. 8, pp. 124–140. DOI: 10.1007/s40789-020-00346-9.
11. Owunna I., Ikpe A.E. Modelling and prediction of the mechanical properties of TIG welded joint for AISI 4130 low carbon steel plates using artificial neural network (ANN) approach. *Nigerian Journal of Technology (NIJOTECH)*, 2019, vol. 38, no. 1, pp. 117–126. DOI: 10.4314/njt.v38i1.16.
12. Mahmoodi-Babolan N., Heydari A., Nematollahzadeh A. Removal of methylene blue via bioinspired catecholamine/starch superadsorbent and the efficiency prediction by response surface methodology and artificial neural network-particle swarm optimization. *Bioresource Technology*, 2019, vol. 294, article number 122084. DOI: 10.1016/j.biortech.2019.122084.
13. Prasad M., Kempaiah U.N., Mohan R.M., Nagaral M. Microstructure, Tensile and Compression Behavior of AlSi10Mg Alloy Developed by Direct Metal Laser Sintering. *Indian Journal of Science and Technology*, 2021, vol. 14, no. 45, pp. 3346–3353. DOI: 10.17485/IJST/v14i45.1705.
14. Zhuo Longchao, Wang Zeyu, Zhang Hongjia, Yin Enhuai, Wang Yanlin, Xu Tao, Li Chao. Effect of post-process heat treatment on microstructure and properties of selective laser melted AlSi10Mg alloy. *Materials Letters*, 2019, vol. 234, pp. 196–200. DOI: 10.1016/j.matlet.2018.09.109.
15. Mei Jiahe, Han Ying, Zu Guoqing, Zhu Weiwei, Zhao Yu, Chen Hua, Ran Xu. Achieving Superior Strength and Ductility of AlSi10Mg Alloy Fabricated by Selective Laser Melting with Large Laser Power and High Scanning Speed. *Acta Metallurgica Sinica (English Letters)*, 2022, vol. 35, pp. 1665–1672. DOI: 10.1007/s40195-022-01410-w.
16. Zhou Suyuan, Su Yang, Gu Rui, Wang Zhenyu, Zhou Yinghao, Ma Qian, Yan Ming. Impacts of Defocusing Amount and Molten Pool Boundaries on Mechanical Properties and Microstructure of Selective Laser Melted AlSi10Mg. *Materials*, 2019, vol. 12, no. 1, article number 73. DOI: 10.3390/ma12010073.
17. Zhang Shuzhe, Wei Pei, Chen Zhen, Li Bobo, Huang Ke, Zou Yatong, Lu Bingheng. Graphene/ZrO_2/aluminum alloy composite with enhanced strength and ductility fabricated by laser powder bed fusion. *Journal of Alloys and Compounds*, 2022, vol. 910, article number 164941. DOI: 10.1016/j.jallcom.2022.164941.
18. Wei Pei, Chen Zhen, Zhang Shuzhe, Li Bobo, Han Jiang, Lu Bingheng. Microstructure and mechanical properties of graphene and nano-zirconia reinforced AlSi10Mg composite fabricated by laser powder bed fusion. *Materials Science and Engineering: A*, 2023, vol. 864, article number 144574. DOI: 10.1016/j.msea.2022.144574.
19. Amor N., Noman M.T., Ismail A., Petru M., Sebastian N. Use of an Artificial Neural Network for Tensile Strength Prediction of Nano Titanium Dioxide Coated Cotton. *Polymers*, 2022, vol. 14, no. 5, article number 937. DOI: 10.3390/polym14050937.
20. Khan A.Q., Awan H.A., Rasul M., Siddiqi Z.A., Pimanmas A. Optimized artificial neural network model for accurate prediction of compressive strength of normal and high strength concrete. *Cleaner Materials*, 2023, vol. 10, article number 100211. DOI: 10.1016/j.clema.2023.100211.

СПИСОК ЛИТЕРАТУРЫ

1. Rouf S., Malik A., Singh N., Raina A., Naveed N., Siddiqui M.I.H., Haq M.I.Ul. Additive manufacturing technologies: Industrial and medical applications // Sustainable Operations and Computers. 2022. Vol. 3. P. 258–274. DOI: 10.1016/j.susoc.2022.05.001.
2. Sercombe T.B., Li X. Selective laser melting of aluminium and aluminium metal matrix composites: review // Materials Technology. 2016. Vol. 31. № 2. P. 77–85. DOI: 10.1179/1753555715Y.0000000078.
3. Chowdhury S., Yadaiah N., Prakash Ch., Ramakrishna S., Dixit S., Gulta L.R., Buddhi D. Laser Powder Bed Fusion: A State-of-the-Art Review of the Technology, Materials, Properties & Defects, and Numerical Modelling // Journal of Materials Research and Technology. 2022. Vol. 20. P. 2109–2172. DOI: 10.1016/j.jmrt.2022.07.121.
4. Xu Yongjun, Liu Xin, Cao Xin et al. Artificial intelligence: A powerful paradigm for scientific research // The Innovation. 2021. Vol. 2. № 4. Article number 100179. DOI: 10.1016/j.xinn.2021.100179.
5. Osman E.-S., Aggour M.A. Artificial neural network model for accurate prediction of pressure drop in horizontal and near-horizontal-multiphase flow // Petroleum Science and Technology. 2002. Vol. 20. № 1-2. P. 1–15. DOI: 10.1081/LFT-120002082.
6. Shubham P., Sharma A., Vishwakarma P.N., Phanden R.K. Predicting Strength of Selective Laser Melting 3D Printed AlSi10Mg Alloy Parts by Machine Learning Models // 8th International Conference on Signal Processing and Integrated Networks (SPIN). India, 2021. P. 745–749. DOI: 10.1109/SPIN52536.2021.9566142.
7. Ghetiya N.D., Patel K.M. Prediction of Tensile Strength in Friction Stir Welded Aluminium Alloy Using Artificial Neural Network // Procedia Technology. 2014. Vol. 14. P. 274–281. DOI: 10.1016/j.protcy.2014.08.036.
8. Khalefa M. Use of artificial neural network for prediction of mechanical properties of Al–Si alloys synthesized by stir casting // Journal of Petroleum and Mining Engineering. 2019. Vol. 21. P. 97–103. DOI: 10.21608/jpme.2019.13857.1004.
9. Alamri F., Maalouf M., Barsoum I. Prediction of Porosity, Hardness and Surface Roughness in Additive Manufactured AlSi10Mg Samples: preprint. 2023. DOI: 10.21203/rs.3.rs-3186551/v1.
10. Lawal A.I., Aladejari A.E., Onifade M., Bada S., Idris M.A. Predictions of elemental composition of coal and biomass from their proximate analyses using ANFIS, ANN and MLR // International Journal of Coal Science and Technology. 2024. Vol. 8. P. 124–140. DOI: 10.1007/s40789-020-00346-9.
11. Owunna I., Ikpe A.E. Modelling and prediction of the mechanical properties of TIG welded joint for AISI 4130 low carbon steel plates using artificial neural network (ANN) approach // Nigerian Journal of Technology (NIJOTECH). 2019. Vol. 38. № 1. P. 117–126. DOI: 10.4314/njt.v38i1.16.
12. Mahmoodi-Babolan N., Heydari A., Nematollahzadeh A. Removal of methylene blue via bioinspired catecholamine/starch superadsorbent and the efficiency prediction by response surface methodology and artificial neural network-particle swarm optimization // Bioresource Technology. 2019. Vol. 294. Article number 122084. DOI: 10.1016/j.biortech.2019.122084.
13. Prasad M., Kempaiah U.N., Mohan R.M., Nagaral M. Microstructure, Tensile and Compression Behavior of AlSi10Mg Alloy Developed by Direct Metal Laser Sintering // Indian Journal of Science and Technology. 2021. Vol. 14. № 45. P. 3346–3353. DOI: 10.17485/IJST/v14i45.1705.
14. Zhuo Longchao, Wang Zeyu, Zhang Hongjia, Yin Enhuai, Wang Yanlin, Xu Tao, Li Chao. Effect of post-process heat treatment on microstructure and properties of selective laser melted AlSi10Mg alloy // Materials Letters. 2019. Vol. 234. P. 196–200. DOI: 10.1016/j.matlet.2018.09.109.
15. Mei Jiahe, Han Ying, Zu Guoqing, Zhu Weiwei, Zhao Yu, Chen Hua, Ran Xu. Achieving Superior Strength and Ductility of AlSi10Mg Alloy Fabricated by Selective Laser Melting with Large Laser Power and High Scanning Speed // Acta Metallurgica Sinica (English Letters). 2022. Vol. 35. P. 1665–1672. DOI: 10.1007/s40195-022-01410-w.
16. Zhou Suyuan, Su Yang, Gu Rui, Wang Zhenyu, Zhou Yinghao, Ma Qian, Yan Ming. Impacts of Defocusing Amount and Molten Pool Boundaries on Mechanical Properties and Microstructure of Selective Laser Melted AlSi10Mg // Materials. 2019. Vol. 12. № 1. Article number 73. DOI: 10.3390/ma12010073.
17. Zhang Shuzhe, Wei Pei, Chen Zhen, Li Bobo, Huang Ke, Zou Yatong, Lu Bingheng. Graphene/ZrO_2/aluminum alloy composite with enhanced strength and ductility fabricated by laser powder bed fusion // Journal of Alloys and Compounds. 2022. Vol. 910. Article number 164941. DOI: 10.1016/j.jallcom.2022.164941.
18. Wei Pei, Chen Zhen, Zhang Shuzhe, Li Bobo, Han Jiang, Lu Bingheng. Microstructure and mechanical properties of graphene and nano-zirconia reinforced AlSi10Mg composite fabricated by laser powder bed fusion // Materials Science and Engineering: A. 2023. Vol. 864. Article number 144574. DOI: 10.1016/j.msea.2022.144574.
19. Amor N., Noman M.T., Ismail A., Petru M., Sebastian N. Use of an Artificial Neural Network for Tensile Strength Prediction of Nano Titanium Dioxide Coated Cotton // Polymers. 2022. Vol. 14. № 5. Article number 937. DOI: 10.3390/polym14050937.
20. Khan A.Q., Awan H.A., Rasul M., Siddiqi Z.A., Pimanmas A. Optimized artificial neural network model for accurate prediction of compressive strength of normal and high strength concrete // Cleaner Materials. 2023. Vol. 10. Article number 100211. DOI: 10.1016/j.clema.2023.100211.

Математическая модель прогнозирования предела прочности сплава AlSi10Mg, изготовленного аддитивным способом, с использованием искусственных нейронных сетей

Шривастава Сунита К.*[1], научный сотрудник кафедры машиностроения
Мативанан Н. Раджеш[2], кандидат наук, профессор кафедры машиностроения
Общественный университет народного просвещения, Бангалор (Индия)

***E-mail:** sunita.shri45@gmail.com

[1]ORCID: https://orcid.org/0009-0005-2174-2067
[2]ORCID: https://orcid.org/0000-0003-1903-2005

Поступила в редакцию 10.09.2024 *Пересмотрена 29.10.2024* *Принята к публикации 25.11.2024*

Аннотация: Внедрение машинного обучения в аддитивное производство для моделирования реальных результатов может значительно снизить его стоимость за счет селективного производства. В настоящее время существует недостаточно исследований, посвященных разработке модели прогнозирования механических свойств материала. Входные переменные предложенной модели включали ключевые параметры процесса селективной лазерной плавки, такие как мощность лазера, толщина слоя, скорость сканирования и шаг штриховки, на выходе получая предел прочности. Математическая модель на основе искусственной нейронной сети сравнивалась с моделью полиномиальной регрессии второй степени. Надежность обеих моделей дополнительно оценивалась с новыми наборами данных, отличных от тех, которые использовались при разработке математической модели на основе искусственной нейронной сети и модели регрессии. Результаты показали, что предложенная математическая модель на основе искусственной нейронной сети обеспечивает превосходную точность: при прогнозировании прочности сплава AlSi10Mg среднее абсолютное процентное отклонение (MAPE) составило 4,74 %, критерий соответствия R^2=0,898. Математический метод на основе искусственной нейронной сети также показал высокую производительность на новых данных – значение регрессии достигало 0,68. Таким образом, разработанную модель возможно рассматривать как перспективный вариант для прогнозирования предела прочности материала.

Ключевые слова: сплав AlSi10Mg; аддитивное производство; искусственная нейронная сеть (ИНС); машинное обучение; селективная лазерная плавка; математическая модель.

Для цитирования: Шривастава С.К., Мативанан Н.Р. Математическая модель прогнозирования предела прочности сплава AlSi10Mg, изготовленного аддитивным способом, с использованием искусственных нейронных сетей // Frontier Materials & Technologies. 2025. № 1. С. 93–110. DOI: 10.18323/2782-4039-2025-1-71-8.

Appendix 1

1. Raus A.A., Wahab M.S., Shayfull Z., Kamarudin K., Ibrahim M. The Influence of Selective Laser Melting Parameters on Density and Mechanical Properties of AlSi10Mg. *MATEC Web of Conferences*, 2016, vol. 78, article number 01078. DOI: 10.1051/matecconf/20167801078.
2. Prasad M., Kempaiah U.N., Mohan R.M., Nagaral M. Microstructure, Tensile and Compression Behaviour of AlSi10Mg Alloy Developed by Direct Metal Laser Sintering. *Indian Journal of Science and Technology*, 2021, vol. 14, no. 45, pp. 3346–3353. DOI: 10.17485/IJST/v14i45.1705.
3. Nirish M., Rajendra R. Heat Treatment Effect on the Mechanical Properties of AlSi10Mg Produced by Selective Laser Melting. *Journal of Mechanical Engineering Research and Developments*, 2022, vol. 45, no. 2, pp. 19–28. URL: https://www.researchgate.net/publication/360783808_Heat_Treatment_Effect_on_the_Mechanical_Properties_of_AlSi10Mg_Produced_by_Selective_Laser_Melting.
4. Ashwath P., Xavior M.A., Batako A., Jeyapandiarajan P., Joel J. Selective laser melting of Al–Si–10Mg alloy: microstructural studies and mechanical properties assessment. *Journal of Materials Research and Technology*, 2022, vol. 17, pp. 2249–2258. DOI: 10.1016/j.jmrt.2022.01.135.
5. Casati R., Hamidi Nasab M., Coduri M., Tirelli V., Vedani M. Effects of Platform Pre-Heating and Thermal-Treatment Strategies on Properties of AlSi10Mg Alloy Processed by Selective Laser Melting. *Metals*, 2018, vol. 8, no. 11, article number 954. DOI: 10.3390/met8110954.
6. Chen B., Moon S.K., Yao X., Bi G., Shen J., Umeda J., Kondoh K. Strength and strain hardening of a selective laser melted AlSi10Mg alloy. *Scripta Materialia*, 2017, vol. 141, pp. 45–49. DOI: 10.1016/j.scriptamat.2017.07.025.
7. Delahaye J., Tchoufang Tchuindjang J., Lecomte-Beckers J., Rigo O., Habraken A.M., Mertens A. Influence of Si precipitates on fracture mechanisms of AlSi10Mg parts processed by Selective Laser Melting. *Acta Materialia*, 2019, vol. 175, pp. 160–170. DOI: 10.1016/j.actamat.2019.06.013.
8. Hitzler L., Janousch C., Schanz J., Merkel M., Heine B., Mack F., Hall W., Öchsner A. Direction and location dependency of selective laser melted AlSi10Mg specimens. *Journal of Materials Processing Technology*, 2017, vol. 243, pp. 48–61. DOI: 10.1016/j.jmatprotec.2016.11.029.
9. John M.D., Flaviana C., Paolo A.E. et al. Direct Metal Laser Sintering: an additive manufacturing technology ready to produce lightweight structural parts for robotic applications. *Politecnico di Torino*. URL: https://iris.polito.it/handle/11583/2518303.

10. Li Wei, Li Shuai, Liu Jie, Zhang Ang, Zhou Yan, Wei Qingsong, Yan Chunze, Shi Yusheng. Effect of heat treatment on AlSi10Mg alloy fabricated by selective laser melting: Microstructure evolution, mechanical properties and fracture mechanism. *Materials Science and Engineering: A*, 2016, vol. 663, pp. 116–125. DOI: 10.1016/j.msea.2016.03.088.
11. Rosenthal I., Stern A., Frage N. Strain rate sensitivity and fracture mechanism of AlSi10Mg parts produced by Selective Laser Melting. *Materials Science and Engineering: A*, 2017, vol. 682, pp. 509–517. DOI: 10.1016/j.msea.2016.11.070.
12. Tang M., Pistorius P.C. Anisotropic Mechanical Behavior of AlSi10Mg Parts Produced by Selective Laser Melting. *JOM*, 2017, vol. 69, pp. 516–522. DOI: 10.1007/s11837-016-2230-5.
13. Wang Lianfeng, Sun Jing, Zhu Xiaogang, Cheng Lingyu, Shi Yun, Guo Lijie, Yan Biao. Effects of T2 Heat Treatment on Microstructure and Properties of the Selective Laser Melted Aluminum Alloy Samples. *Materials*, 2018, vol. 11, no. 1, article number 66. DOI: 10.3390/ma11010066.
14. Zhuo Longchao, Wang Zeyu, Zhang Hongjia, Yin Enhuai, Wang Yanlin, Xu Tao, Li Chao. Effect of post-process heat treatment on microstructure and properties of selective laser melted AlSi10Mg alloy. *Materials Letters*, 2019, vol. 234, pp. 196–200. DOI: 10.1016/j.matlet.2018.09.109.
15. Larrosa N.O., Wang W., Read N., Loretto M.H., Evans C., Carr J., Tradowsky U., Attallah M.M., Withers P.J. Linking microstructure and processing defects to mechanical properties of selectively laser melted AlSi10Mg alloy. *Theoretical and Applied Fracture Mechanics*, 2018, vol. 98, pp. 123–133. DOI: 10.1016/j.tafmec.2018.09.011.
16. Manfredi D., Calignano F., Krishnan M., Canali R., Ambrosio E.P., Atzeni E. From Powders to Dense Metal Parts: Characterization of a Commercial AlSiMg Alloy Processed through Direct Metal Laser Sintering. *Materials*, 2013, vol. 6, no. 3, pp. 856–869. DOI: 10.3390/ma6030856.
17. Ming Tang, Pistorius P.C. Oxides, porosity and fatigue performance of AlSi10Mg parts produced by selective laser melting. *International Journal of Fatigue*, 2017, vol. 94, part 2, pp. 192–201. DOI: 10.1016/j.ijfatigue.2016.06.002.
18. Mei Jiahe, Han Ying, Zu Guoqing, Zhu Weiwei, Zhao Yu, Chen Hua, Ran Xu. Achieving Superior Strength and Ductility of AlSi10Mg Alloy Fabricated by Selective Laser Melting with Large Laser Power and High Scanning Speed. *Acta Metallurgica Sinica*, 2022, vol. 35, pp. 1665–1672. DOI: 10.1007/s40195-022-01410-w.
19. Zyguła K., Nosek B., Pasiowiec H., Szysiak N. Mechanical properties and microstructure of AlSi10Mg alloy obtained by casting and SLM technique. *World Scientific News*, 2018, vol. 104, pp. 462–472. URL: https://www.researchgate.net/publication/330215508_Mechanical_properties_and_microstructure_of_AlSi10Mg_alloy_obtained_by_casting_and_SLM_technique.
20. Hovig E.W., Azar A.S., Mhamdi M., Sørby K. Mechanical Properties of AlSi10Mg Processed by Laser Powder Bed Fusion at Elevated Temperature. *TMS 2020 149th Annual Meeting & Exhibition Supplemental Proceedings*. London, Springer Cham Publ., 2020, pp. 395–404. DOI: 10.1007/978-3-030-36296-6_37.
21. Zhou Suyuan, Su Yang, Gu Rui, Wang Zhenyu, Zhou Yinghao, Ma Qian, Yan Ming. Impacts of Defocusing Amount and Molten Pool Boundaries on Mechanical Properties and Microstructure of Selective Laser Melted AlSi10Mg. *Materials*, 2019, vol. 12, no. 1, article number 73. DOI: 10.3390/ma12010073.
22. Tan Qiyang, Yin Yu, Fan Zhiqi, Zhang Jingqi, Liu Yingang, Zhang Ming-Xing. Uncovering the roles of LaB6-nanoparticle inoculant in the AlSi10Mg alloy fabricated via selective laser melting. *Materials Science and Engineering: A*, 2021, vol. 800, article number 140365. DOI: 10.1016/j.msea.2020.140365.
23. Famodimu O.H., Stanford M., Oduoza C.F., Lijuan Zhang. Effect of process parameters on the density and porosity of laser melted AlSi10Mg/SiC metal matrix composite. *Frontiers of Mechanical Engineering*, 2018, vol. 13, pp. 520–527. DOI: 10.1007/s11465-018-0521-y.
24. Marchese G., Aversa A., Lorusso M., Manfredi D., Calignano F., Lombardi M., Biamino S., Pavese M. Development and Characterisation of Aluminium Matrix Nanocomposites AlSi10Mg/$MgAl_2O_4$ by Laser Powder Bed Fusion. *Metals*, 2018, vol. 8, no. 3, article number 175. DOI: 10.3390/met8030175.
25. Gao C., Wu W., Shi J., Xiao Z., Akbarzadeh A.H. Simultaneous enhancement of strength, ductility, and hardness of TiN/AlSi10Mg nanocomposites via selective laser melting. *Additive Manufacturing*, 2020, vol. 34, article number 101378. DOI: 10.1016/j.addma.2020.101378.
26. He Peidong, Kong Hui, Liu Qian, Ferry M., Kruzic J.J., Li Xiaopeng. Elevated temperature mechanical properties of TiCN reinforced AlSi10Mg fabricated by laser powder bed fusion additive manufacturing. *Materials Science and Engineering: A*, 2021, vol. 811, article number 141025. DOI: 10.1016/j.msea.2021.141025.
27. Wang Yachao, Shi Jing, Lu Shiqiang, Xiao Weihan. Investigation of Porosity and Mechanical Properties of Graphene Nanoplatelets-Reinforced AlSi10Mg by Selective Laser Melting. *Journal of Micro and Nano Science and Engineering*, 2018, vol. 6, no. 1, article number 010902. DOI: 10.1115/1.4038454.
28. Wang Yachao, Shi Jing. Effect of hot isostatic pressing on nanoparticles reinforced AlSi10Mg produced by selective laser melting. *Materials Science and Engineering: A*, 2020, vol. 788, article number 139570. DOI: 10.1016/j.msea.2020.139570.
29. Wei Pei, Chen Zhen, Zhang Shuzhe, Li Bobo, Han Jiang, Lu Bingheng. Microstructure and mechanical properties of graphene and nano-zirconia reinforced AlSi10Mg composite fabricated by laser powder bed fusion. *Materials Science and Engineering: A*, 2023, vol. 864, article number 144574. DOI: 10.1016/j.msea.2022.144574.
30. Zhang Shuzhe, Chen Zhen, Wei Pei et al. Wear properties of graphene/zirconia biphase nano-reinforced aluminium matrix composites prepared by SLM. *Materials Today Communications*, 2022, vol. 30, article number 103009. DOI: 10.1016/j.mtcomm.2021.103009.
31. Zhang Shuzhe, Wei Pei, Chen Zhen, Li Bobo, Huang Ke, Zou Yatong, Lu Bingheng. Graphene/ZrO_2/aluminum alloy composite with enhanced strength and ductility fabricated by laser powder bed fusion. *Journal of Alloys and Compounds*, 2022, vol. 910, article number 164941. DOI: 10.1016/j.jallcom.2022.164941.
32. Yi Junchao, Zhang Xiaowei, Rao Jeremy Heng, Xiao Jingyu, Jiang Yehua. In-situ chemical reaction mechanism and non-equilibrium microstructural evolution of (TiB2 + TiC)/AlSi10Mg composites prepared by SLM-CS processing. *Journal of Alloys and Compounds*, 2021, vol. 857, article number 157553. DOI: 10.1016/j.jallcom.2020.157553.
33. Miao Kai, Zhou Hang, Gao Yunpeng, Deng Xin, Lu Zhongliang, Li Dichen. Laser powder-bed-fusion of Si_3N_4 reinforced AlSi10Mg composites: Processing, mechanical properties and strengthening mechanisms. *Materials Science and Engineering: A*, 2021, vol. 825, article number 141874. DOI: 10.1016/j.msea.2021.141874.

34. Limbasiya N., Jain A., Soni H., Wankhede V., Krolczyk G., Sahlot R. A comprehensive review on the effect of process parameters and post-process treatments on microstructure and mechanical properties of selective laser melting of AlSi10Mg. *Journal of Materials Research and Technology*, 2022, vol. 21, pp. 1141–1176. DOI: 10.1016/j.jmrt.2022.09.092.

Appendix 2

1. Maamoun A.H., Xue Y.F., Elbestawi M.A., Veldhuis S.C. The Effect of Selective Laser Melting Process Parameters on the Microstructure and Mechanical Properties of Al6061 and AlSi10Mg Alloys. *Materials*, 2019, vol. 12, no. 1, article number 12. DOI: 10.3390/ma12010012.
2. Srinivasa Rakesh Ch., Raja A., Nadig P., Jayaganthan R., Vasa N.J. Influence of working environment and built orientation on the tensile properties of selective laser melted AlSi10Mg alloy. *Materials Science and Engineering: A*, 2019, vol. 750, pp. 141–151. DOI: 10.1016/j.msea.2019.01.103.
3. Dong Zhichao, Zhang Xiaoyu, Shi Wenhua, Zhou Hao, Lei Hongshuai, Liang Jun. Study of Size Effect on Microstructure and Mechanical Properties of AlSi10Mg Samples Made by Selective Laser Melting. *Materials*, 2018, vol. 11, no. 12, article number 2463. DOI: 10.3390/ma11122463.
4. Li Xinwei, Shi Shi, Han Shuang, Hu Xiaogang, Zhu Qiang, Lu Hongxing, Li Wenwu, Shi Yusheng, Ding Hui. Microstructure, solidification behavior and mechanical properties of Al-Si-Mg-Ti/TiC fabricated by selective laser melting. *Additive Manufacturing*, 2020, vol. 34, article number 10132. DOI: 10.1016/j.addma.2020.101326.
5. Kempen K., Thijs L., Van Humbeeck J., Kruth J.-P. Processing AlSi10Mg by selective laser melting: parameter optimisation and material characterisation. *Materials Science and Technology*, 2014, vol. 31, no. 8, pp. 917–923. DOI: 10.1179/1743284714Y.0000000702.
6. Kim Dong-Kyu, Woo Wanchuck, Hwang Ji-Hyun, An Ke, Choi Shi-Hoon. Stress partitioning behavior of an AlSi10Mg alloy produced by selective laser melting during tensile deformation using in situ neutron diffraction. *Journal of Alloys and Compounds*, 2016, vol. 686, pp. 281–286. DOI: 10.1016/j.jallcom.2016.06.011.
7. Maskery I., Aboulkhair N.T., Tuck C.J., Wildman R., Ashcroft I., Everitt N.M., Hague R.J.M.. Fatigue Performance Enhancement of Selectively Laser Melted Aluminium Alloy by Heat Treatment. *26th Annual International Solid Freeform Fabrication Symposium*. Texas, 2015, pp. 1–10. URL: https://www.researchgate.net/publication/282816647_Fatigue_Performance_Enhancement_of_Selectively_Laser_Melted_Aluminium_Alloy_by_Heat_Treatment.
8. Sun Jing, Qiu Lianfang, Wang Fei, Yang Yang, Guo Lijie. A new modification effect of eutectic Si in selective laser melted AlSi10Mg. *Materials Science and Technology*, 2019, vol. 35, no. 6, pp. 1–7. DOI: 10.1080/02670836.2019.1589740.
9. Wei Pei, Wei Zhengying, Chen Zhen, Du Jun, He Yuyang, Li Junfeng, Zhou Yatong. The AlSi10Mg samples produced by selective laser melting: single track, densification, microstructure and mechanical behaviour. *Applied Surface*, 2017, vol. 408, pp. 38–50. DOI: 10.1016/j.apsusc.2017.02.215.
10. Zhang Changchun, Zhu Haihong, Liao Hailong, Cheng Yong, Hu Zhiheng, Zeng Xiaoyan. Effect of heat treatments on fatigue property of selective laser melting AlSi10Mg. *International Journal of Fatigue*, 2018, vol. 116, pp. 513–522. DOI: 10.1016/j.ijfatigue.2018.07.016.
11. Yang Tao, Liu Tingting, Liao Wenhe, MacDonald E., Wei Huiliang, Zhang Changdong, Chen Xiangyuan, Zhang Kai. Laser powder bed fusion of AlSi10Mg: Influence of energy intensities on spatter and porosity evolution, microstructure and mechanical properties. *Journal of Alloys and Compounds*, 2020, vol. 849, article number 156300. DOI: 10.1016/j.jallcom.2020.156300.
12. Yan Qian, Song Bo, Shi Yusheng. Comparative study of performance comparison of AlSi10Mg alloy prepared by selective laser melting and casting. *Journal of Materials Science & Technology*, 2020, vol. 41, pp. 199–208. DOI: 10.1016/j.jmst.2019.08.049.
13. Suttey L.J. Evaluation of metallurgical and mechanical properties of AlSi10Mg produced by selective laser melting: Graduate Theses & Non-Theses. 2018. 174. *Digital Commons and Montana Tech*. URL: https://digitalcommons.mtech.edu/grad_rsch/174.
14. Liu Bin, Kuai Zezhou, Li Zhonghua, Tong Jianbin, Bai Peikang, Li Baoqiang, Nie Yunfei. Performance Consistency of AlSi10Mg Alloy Manufactured by Simulating Multi Laser Beam Selective Laser Melting (SLM): Microstructures and Mechanical Properties. *Materials*, 2018, vol. 11, no. 12, article number 2354. DOI: 10.3390/ma11122354.
15. Murphy D.M. Performance evaluation of AlSi10Mg fabricated by a selective laser melting process. *Missouri University of Science and Technology*. URL: https://scholarsmine.mst.edu/masters_theses/8006.
16. Kumar M.S., Mohan E., Robinson S., Prasad T.D. Comparative Study on Morphological, Physical and Mechanical Characteristics of L-PBF Based AlSi10Mg Parts with Conventional Stir Casted Al-10%SiC Composites. *Silicon*, 2022, vol. 14, pp. 2695–2706. DOI: 10.1007/s12633-021-01065-9.
17. Zhou S.Y., Wang Z.Y., Su Y., Wang H., Liu G., Song T.T., Yan M. Effects of Micron/Submicron TiC on Additively Manufactured AlSi10Mg: A Comprehensive Study from Computer Simulation to Mechanical and Microstructural Analysis. *JOM*, 2020, vol. 72, pp. 3693–3704. DOI: 10.1007/s11837-019-03984-w.